DFUB 27/92

SELECTED RESULTS FROM THE OPAL EXPERIMENT AT LEP

Fermilab Library
0 1160 0019970 7

G. Giacomelli

Dipartimento di Fisica dell'Università di Bologna, Italy
CERN, Geneva, Switzerland
INFN, Sezione di Bologna, Italy

ABSTRACT

This paper describe the OPAL detector at LEP (CERN) and some of the results obtained during the first years of operation. In particular, the results on the Z^0 line shape, leptonic decays and multihadronic final states are discussed.

*)The OPAL Collaboration comprises:
Univ. Birmingham, UK
Univ. Bologna, Italy
Univ. Bonn, Germany
Univ. Cambridge, UK
Univ. California, Riverside, Calif., USA
Carleton Univ., Ottawa, Canada
CERN, Geneva, Switzerland
Univ. Chicago, Ill., USA
Albert-Ludwigs-Univ., Freiburg, Germany
University of Hamburg/DESY, Hamburg, Germany
Univ. Heidelberg, Germany
Indiana Univ, Bloomington, Indiana, USA
Birkbeck College, London, UK
Queen Mary College, London, UK
Univ. College London, UK
Univ. Manchester, UK
Univ. Maryland, College Park, Md., USA
Univ. Montreal, Canada
Nat. Res. Council, Ottawa, Canada
Rutherford Appleton Lab., UK
CEN-Saclay, France
Technion-Israel Inst. of Technology, Haifa, Israel
Tel Aviv Univ., Israel
Univ. Tokyo, Japan
Brunel University, Uxbridge, UK
University of British Columbia, Vancouver, Canada
University of Victoria, Victoria, Canada
Weizmann Inst., Rehovot, Israel

1. INTRODUCTION

Since August 1989, the new Large Electron–Positron Collider (LEP) [1] is operating at CERN. In the period 1989–1991, the four experiments [2] at LEP (ALEPH, DELPHI, L3, and OPAL) recorded over two million events, corresponding to an integrated luminosity of 19.2 pb^{-1}. (OPAL recorded 590,000 events of which 530,000 were multi-hadronic).

The main purposes of the physics [3, 4] at LEP may be broadly classified as follows:

i) precision tests of the Standard Model of the electroweak and strong interactions;
ii) searches for the still missing items of the Standard Model (Higgs boson, top quark);
iii) searches for new physics beyond the Standard Model (supersymmetric particles, subconstituents, etc.);
iv) detailed studies of QCD.

LEP is now working at energies at or around the Z^0 mass, about 50 GeV per beam (this phase is usually referred to as LEP-1 or LEP-100). Since the Z^0 is a carrier of the weak force, the precise measurements of its mass, width, and decay properties provide precision tests of the electroweak theory. The mass of the Z^0 is a fundamental parameter of this theory. The width of the Z^0 peak is a measure of the Z^0 lifetime, which in turn depends on the total number of decay modes available. In the Standard Model the Z^0 decay width is directly connected with the number of fermion pairs into which the Z^0 can decay. The more ways in which it can decay, the faster it decays and the wider the Z^0 peak becomes. A precise measurement of the Z^0 width constrains the number of generations, and a deviation from an integer value will give hints of new physics.

Radiative corrections modify the Breit–Wigner shape of the Z^0 resonance, reducing its height by 30%, shifting its position a little, and making the shape slightly asymmetric.

Since the Z^0 decays predominantly into quark–antiquark pairs, it yields a clean data sample with which to test quantum chromodynamics (QCD), the theory of the strong interaction. The quark–antiquark pair is never observed directly, but it gives rise to two opposite jets of hadrons, by a process called fragmentation. Before fragmentation takes place, one of the quarks may radiate a gluon by a process similar to bremsstrahlung. In this case, three jets of hadrons are produced. The ratio of the number of three-jet events to the number of two-jet events provides one way to measure α_s, the strong coupling constant, which is a fundamental parameter of QCD. α_s has also been measured by a variety of methods.

In the Standard Model with three families, still missing is the heaviest quark, the top quark (t). The analyses of radiative corrections have given precise limits for the top-quark mass.

In addition to the quarks, the leptons, and the carriers of the interactions, the Standard Model requires at least one scalar Higgs particle (the H^0), which is needed for the hypothesized mechanism for the generation of masses. The coupling of the Higgs particle is predicted by the theory, but not its mass. The production cross-section for the Higgs decreases quickly with increasing Higgs mass. Thus the search for the Higgs boson will become progressively more difficult.

Searches for new physics include searches for supersymmetric particles, charged Higgs bosons, substructures of quarks and leptons, excited leptons, tests of various conservation laws, and so on.

These notes will discuss the LEP accelerator and its present performance, the OPAL detector [5], and some of the experimental results obtained by OPAL.

2. LEP

Table 1 gives the main parameters of LEP [1], and Fig. 1 shows the general LEP layout.

Table 1

Main parameters of LEP 1.
LEP 2 will reach 100 GeV per beam and higher luminosities

Energy per beam (GeV)	50
Circumference (m)	26658
Radius of curvature (m)	3096
Injection energy (GeV)	20
No. of e^+ (and e^-) bunches	4
Maximum luminosity (cm^{-2} s^{-1})	1.7×10^{31}
Time separation between crossings (μs)	22.2
e^- (e^+) beam current (mA)	3
Bunch dimensions at intersection: $\sigma_h(\mu m)$	300
$\sigma_v(\mu m)$	20
$4\ \sigma_Z$ (cm)	5
No. of dipoles	3304
Magnetic field (G)	215–600
No. of quadrupoles (sextupoles)	816 (54)
RF frequency (MHz)	352.21
Accelerating power (MW)	10
Energy loss (by synchrotron radiation) (MeV per turn)	260

The standard setting-up procedure for LEP is the following: A high-intensity beam of electrons, accelerated to 200 MeV, hits a high-Z target, where positrons are produced. The positrons are accelerated to 600 MeV in the LEP Injector Linacs (LIL). They are then accumulated in eight bunches in the Electron–Positron Accumulator (EPA), where they are 'naturally' cooled by synchrotron radiation. The positrons are then transferred to the Proton Synchrotron (PS), where they are accelerated to 3.5 GeV. Then the Super Proton Synchrotron (SPS) accelerates them to 20 GeV. The eight bunches are finally transferred to the LEP ring where they are reassembled into four bunches. This procedure is repeated for electrons (600 MeV in LIL and then, in the opposite direction, 3.5 GeV in the PS, 20 GeV in the SPS, and 20 GeV in LEP). In the next phase, positrons and electrons in LEP are

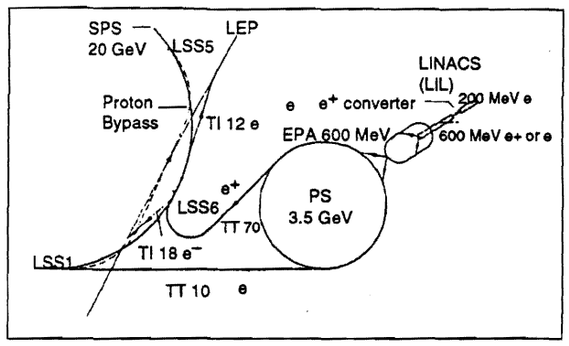

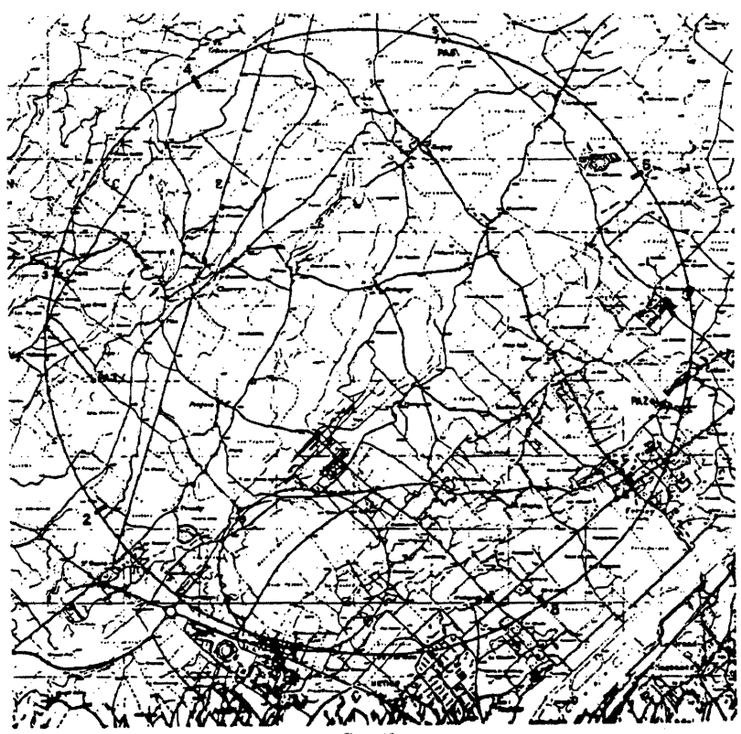

Figure 1: The injectors for LEP and general layout of LEP. OPAL is located at point 6.

accelerated together to the desired energy, say 46 GeV per beam. The whole sequence takes at least one hour. As soon as the beams are reasonably stable, the superconducting quadrupoles at each interaction region are turned on: they reduce the transverse dimensions of each beam to 300 μm $\times$ 20 μm r.m.s. The bunches are also squeezed in length to about $\sigma_z = 13$ mm ($4\sigma_z = 5$ cm total).

Lastly, sets of collimators are positioned; LEP is then ready for physics. The initial luminosity has increased steadily to about 7×10^{30} cm^{-2} s^{-1}. After about ten hours, when the luminosity is reduced to about one quarter, the beams are dumped and the whole operation is repeated.

Recently operation with 8 bunches per beam has been tried succesfully.

3. THE OPAL DETECTOR

OPAL [5] has been built by a collaboration of 28 research institutes from Europe, the Middle East, North America, and Japan; new collaborators joined later. Work started on detector development and design studies in 1981, and six years were needed in which to build, calibrate, and assemble the detector parts. It has cost about 70 million Swiss francs, weighs about 3000 t, has a cylindrical shape of about 8 m diameter and 10 m length (Fig. 2), and is placed in a large underground experimental hall of the LEP collider complex.

OPAL consists of 15 'independent' detectors, whose combined role is to measure, with high precision, the energy, direction, charge, and type of the particles produced. Apart from neutrinos, no particle should be able to escape from the detector without leaving some sign of its passage. A solenoid magnet deflects the charged particles so that their electric charge and momentum can be derived from their measured curved trajectories. The interaction region is surrounded in sequence by detectors, all with a cylindrical structure, with a 'barrel' and two 'end-caps' and with 4π coverage. Tracking is performed by a Central Detector, whilst electron and photon energy measurements are done by a high-resolution electromagnetic (e.m.) calorimeter using lead-glass Cherenkov counters. The magnet iron yoke is instrumented as a hadron calorimeter. The Forward Detector completes the e.m. coverage by tagging small-angle electrons and photons, and is used as a luminosity monitor.

The data from the subdetectors are collected by means of high-speed electronics: there are over 170,000 channels of information. The data acquisition is activated by a two-level trigger system: a fast trigger (20 ns) and an on-line filter (20 μs). A pretrigger is being implemented in order to cope with a higher number of bunches.

The data are combined and reduced in many electronic units before being conveyed to the surface on a single fibre-optic cable. Here the main computer records and monitors the data.

In order to select and measure the cross-section for a specific channel, one needs

i) a trigger,
ii) the required events (N_i)
iii) the computation of the global efficiency (ϵ_i), and
iv) a luminosity determination ($\int L\, dt$):

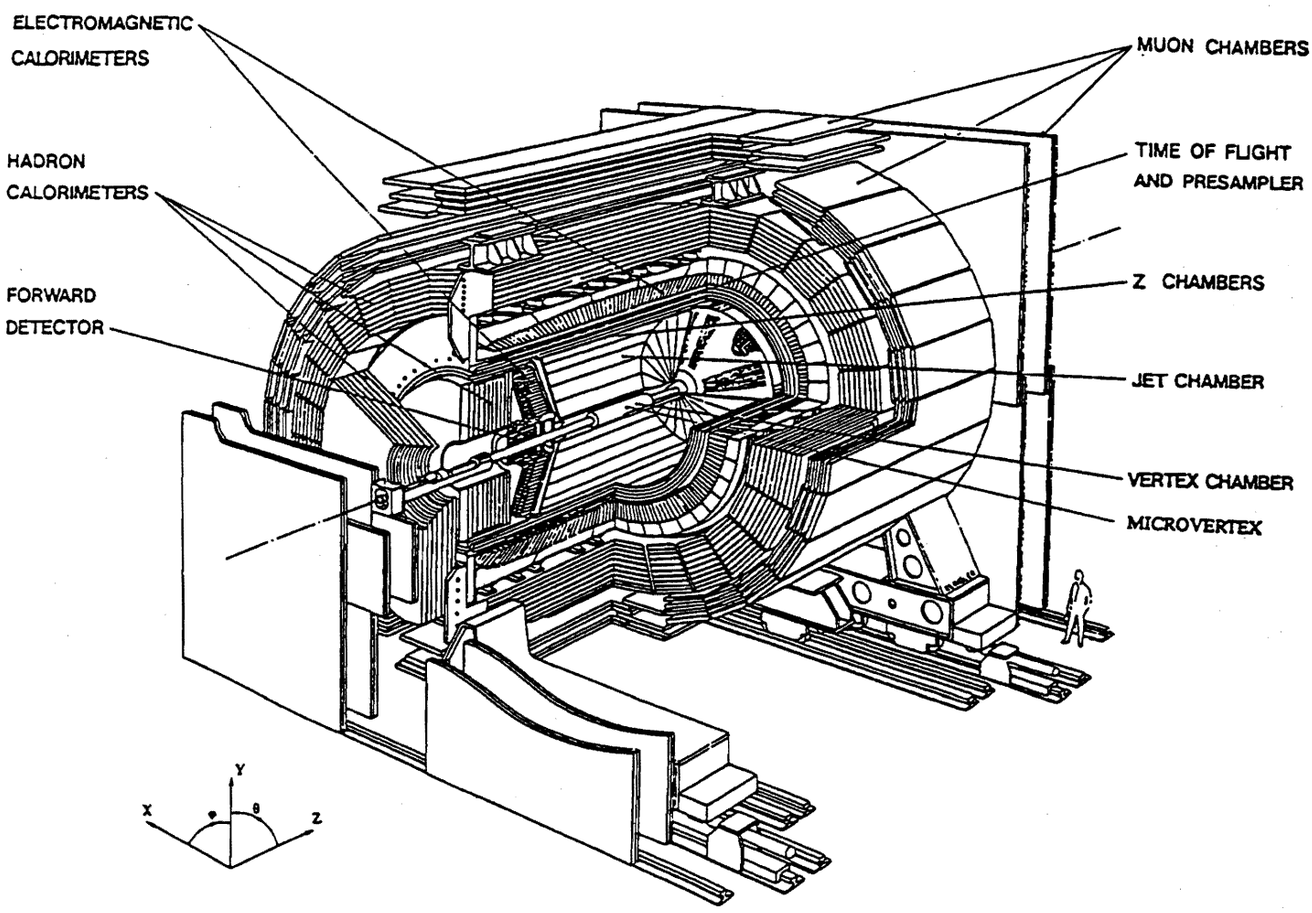

Figure 2: Cut-away of OPAL, with indication of the different detectors.

$$\sigma_i = N_i/(\epsilon_i \int L\, dt) \,. \tag{1}$$

The triggers used by OPAL are all in an OR configuration. The highly redundant triggers imply high triggering efficiencies, greater than 98% for most channels. At present the luminosity determination is limited to a systematic uncertainty of slightly less than 1%. A new luminometer will yield the luminosity to a precision of 0.1%.

The 'events', that is the observed reactions, are particularly simple. A quick scan of the events directly on line is quite instructive and shows that they can be mostly classified as two-body events. The e^+e^-, $\mu^+\mu^-$, $\tau^+\tau^-$ final states (3.4% each), and the rare electromagnetic final state $\gamma\gamma$ are typical two-body events. The most abundant reaction is the two-jet hadron events, in which the two jets are back to back; this is evidence for an underlying simplicity. In fact these events are due to $e^+e^- \to q\bar{q} \to 2$ jets. A closer look shows evidence of a number of almost two-jet events, with a small third jet; there are also clear three-jet events. They are all interpreted as $e^+e^- \to q\bar{q} \to q\bar{q}g \to 3$ jets, where the gluon g is radiated by the quark or the antiquark by a process similar to bremsstrahlung.

4. MASS AND WIDTH OF THE Z^0

4.1 Generalities. The Breit–Wigner Shape.

At the Z^0 peak the basic processes are

$$e^+e^- \to Z^0 \to q\bar{q} \tag{2a}$$

$$\to \ell\bar{\ell}, \tag{2b}$$

where the $q\bar{q}$ pairs are $u\bar{u}$, $d\bar{d}$, $s\bar{s}$, $c\bar{c}$, and $b\bar{b}$ (the $t\bar{t}$ has a higher mass). As already stated, each quark or antiquark hadronizes in a jet of hadrons. Therefore the $q\bar{q}$ pairs are characterized by two opposite jets of hadrons. The quark (and/or the antiquark) may radiate a gluon, which gives rise to a third jet (or more). The $\ell\bar{\ell}$ pairs are either charged (e^+e^-, $\mu^+\mu^-$, $\tau^+\tau^-$) or neutral ($\nu_e\bar{\nu}_e$, $\nu_\mu\bar{\nu}_\mu$, $\nu_\tau\bar{\nu}_\tau$).

The existence of a fourth family of quarks and leptons with masses smaller than half the Z^0 mass would increase the number of open channels, thus increasing the width of the Z^0 (decreasing its lifetime) and lowering the height of the peak cross-section. New physics (such as the existence of supersymmetric particles) may contribute a fraction of the width contributed by each of the three families.

Scans around the Z^0 mass were performed, taking data at seven to eleven energies between 88 and 94 GeV. Most of the data points have been measured many times. The behaviour of the cross-section around the Z^0 peak is typical of a resonant state with $J = 1$ and is well described by a Breit–Wigner formula with an s-dependent width and with radiative corrections:

$$\sigma(s) = \frac{12\pi(\hbar c)^2}{m_Z^2} s \frac{\Gamma_e \Gamma_f}{(s - m_Z^2)^2 + m_Z^2 \Gamma_Z^2} [1 - \delta(s)] \,, \tag{3}$$

where Γ_f ($= \Gamma_{f\bar{f}} = \Gamma_{f\bar{f}}$) is the partial width for the decay of the Z^0 into a fermion–antifermion pair, $Z^0 \to f + \bar{f}$, and δ includes the effects of radiative corrections. The total width Γ_Z is given by

$$\Gamma_Z = \Gamma_h + \Gamma_e + \Gamma_\mu + \Gamma_\tau + N_\nu \Gamma_\nu = \Gamma_{vis} + \Gamma_{invis} \ , \tag{4}$$

where Γ_h is the total hadronic width and $\Gamma_e, \Gamma_\mu, \Gamma_\tau, \Gamma_\nu$ are the leptonic widths. In the Standard Model,

$$\begin{cases} \Gamma_h &= \Gamma_u + \Gamma_d + \Gamma_s + \Gamma_c + \Gamma_b = 1734 \text{ MeV} \\ \Gamma_u &= \Gamma_c = 300 \text{ MeV}, \quad \Gamma_d = \Gamma_s = \Gamma_b = 380 \text{ MeV} \\ \Gamma_e &= \Gamma_\mu = \Gamma_\tau = 83.4 \text{ MeV} \\ \Gamma_\nu &= 166.5 \text{ MeV}, \quad N_\nu = 3, \quad \Gamma_{invis} = 499 \text{ MeV} \\ \Gamma_Z &= \Gamma_h + 3\Gamma_\ell + 3\Gamma_\nu = 2487 \text{ MeV} \end{cases} \tag{5}$$

At $s = m_Z^2$, Eq. (3) yields:

$$\sigma(s = m_Z^2) = \frac{12\pi(\hbar c)^2}{m_Z^2} \frac{\Gamma_e \Gamma_f}{\Gamma_Z^2}(1 - \delta) \ . \tag{6}$$

For $e^+e^- \to Z \to$ hadrons, Eq. (3) gives:

$$\sigma_h(s) = \sigma_h^p \frac{s\Gamma_Z^2}{(s - m_Z^2)^2 + s^2\Gamma_Z^2/m_Z^2} (1 - \delta) \ , \tag{7}$$

where σ_h^p is the pole hadron cross-section:

$$\sigma_h^p = \frac{12\pi(\hbar c)^2 \Gamma_e \Gamma_h}{m_Z^2 \Gamma_Z^2} \ . \tag{8}$$

In order to take into account radiative corrections, the Breit–Wigner formula may be corrected as indicated in Eqs. (3), (6) and (7) or, better still, be convoluted with the initial-state radiation spectrum

$$\sigma(s) = \int_{m_\pi^2}^{s} f(s, s') \bar{\sigma}(s') \, ds' \ . \tag{9}$$

The effect of the radiative corrections is illustrated in Fig. 3. The separation of the different leptonic channels is qualitatively illustrated in Fig. 4.

In the electroweak theory the partial widths Γ_f may be expressed in terms of vector and axial-vector coupling constants:

$$a_f = I_{3f} \ , \quad v_f = I_{3f} - 2Q_f \sin^2\theta_w \ , \tag{10}$$

where I_{3f} is the third component of the weak isospin, Q_f is the electric charge of the fermion and θ_w is the weak mixing angle. At the lowest (tree) order one has:

$$\Gamma_f = N_c \frac{G_\mu \, m_Z^3}{6\sqrt{2}\pi}(v_f^2 + a_f^2) \ , \tag{11}$$

where N_c is the number of colours ($N_c = 1$ for leptons, $N_c = 3$ for quarks).